NASA Technical Memorandum 106927

A Study of Elevated Temperature Testing Techniques for the Fatigue Behavior of PMCS: Application to T650-35/AMB21

Andrew L. Gyekenyesi
Cleveland State University
Cleveland, Ohio

Michael G. Castelli
NYMA, Inc.
Brook Park, Ohio

John R. Ellis
Lewis Research Center
Cleveland, Ohio

Christopher S. Burke
NYMA, Inc.
Brook Park, Ohio

July 1995

National Aeronautics and
Space Administration

A STUDY OF ELEVATED TEMPERATURE TESTINGTECHNIQUES FOR THE FATIGUE BEHAVIOR OF PMCS: APPLICATION TO T650-35/AMB21

Andrew L. Gyekenyesi
Cleveland State University
Cleveland, Ohio 44115

Michael G. Castelli
NYMA, Inc.
Brook Park, Ohio 44142

John R. Ellis
National Aeronautics and Space Administration
Lewis Research Center
Cleveland, Ohio 44135

and

Christopher S. Burke
NYMA, Inc.
Brook Park, Ohio 44142

SUMMARY

An experimental study was conducted to investigate the mechanical behavior of a T650-35/AMB21 eight-harness satin weave polymer composite system. Emphasis was placed on the development and refinement of techniques used in elevated temperature uniaxial PMC testing. Issues such as specimen design, gripping, strain measurement, and temperature control and measurement were addressed. Quasi-static tensile and fatigue properties ($R_\sigma = 0.1$) were examined at room and elevated temperatures. Stiffness degradation and strain accumulation during fatigue cycling were recorded to monitor damage progression and provide insight for future analytical modeling efforts. Accomplishments included an untabbed dog-bone specimen design which consistently failed in the gage section, accurate temperature control and assessment, and continuous in-situ strain measurement capability during fatigue loading at elevated temperatures. Finally, strain accumulation and stiffness degradation during fatigue cycling appeared to be good indicators of damage progression.

INTRODUCTION

Because of their high strength to weight ratio, unique flexibility in design capability, and ease of fabrication, fiber reinforced polymer matrix composites (PMCs) have achieved acceptance as engineering materials in the aerospace industry. Since most aerospace structural applications involve a dynamic environment, the static characteristics as well as the fatigue behavior must be well understood to insure structural integrity and safety. To meet this requirement, extensive mechanical testing and data collection have been completed over the years, although, primarily in a room temperature environment (refs. 1 to 5). However, because of the relatively low use temperature of the employed epoxy matrices in most structural PMCs during the past two decades of their use, the data was deemed sufficient for most applications.

The development of polyimides and other advanced thermoset polymers expanded the role of PMCs to elevated temperatures, such as airframe and propulsion system components where severe operating environ-

ments are encountered. Cost effective and easily processed polyimides, such as PMR-15, have been tested and employed in composites for selected turbofan engine structures (ref. 6). Studies dealing with thermal cycling, static tensile loading, and fatigue cycling of PMR-15 have been published previously (refs. 7 to 11).

Environmental and safety concerns about the processing chemicals of PMR resins have initiated the development of environmentally friendly resins such as AMB21. Because of the suspected carcinogenic effects of MDA (Methylene Di Aniline), which is used in the processing of PMR-15, the resin AMB21 was developed as a non-MDA substitute for PMR-15. The properties of PMR-15 are maintained with only a slight decrease in the glass transition temperature. For this investigation, the AMB21 resin was studied in a woven graphite fiber composite system. The results provided data to help establish AMB21 as a valid and safe substitute for PMR-15.

The use of PMCs in the harsh conditions mentioned above has raised concerns relating to the degradation of the physical properties under simultaneous mechanical and environmental loads. These concerns can be addressed by creating a well documented data base of various experimental situations. There is a significant data base already for quasi-static and fatigue load conditions at room temperature. The effect of environmental factors such as moisture content or radiation on mechanical properties has also been studied for various PMCs (refs. 12 and 13). Temperature, on the other hand, has mostly been a variable in experiments dealing with viscoelastic behavior or the nonmechanical thermal cycling of specimens (refs. 14 and 17). Few studies have been published dealing with the high temperature quasi-static and fatigue behavior of polymer composites (refs. 18 to 20), and fewer still when thermomechanical testing is involved (ref. 21). Because of the limited number of studies and the wide array of objectives, a focused effort is required to develop experimental procedures for elevated temperature uniaxial testing of PMCs.

The objective of this investigation is to develop experimental techniques for elevated temperature, uniaxial mechanical testing of PMCs. To this end, the tensile and cyclic fatigue behavior of a carbon /polyimide eight-harness satin weave system, T650-35/AMB21 were investigated. Issues such as optimal specimen design, strain assessment techniques, and temperature measurement methods for quartz lamp heating were examined. Finally, the subject of a measurable damage metric was addressed. Test procedures were implemented to measure the stiffness degradation and strain ratcheting which occurred during the fatigue tests. Such data is considered as fundamental input for future life prediction modeling efforts.

EXPERIMENTAL DETAILS

The laboratory arrangement was constructed for the purpose of testing PMCs at elevated temperatures. Quartz lamps were employed as the heat source due to their dynamic capability. This capacity allows for quick temperature changes that will accommodate future thermomechanical fatigue studies. Concerns, such as temperature measurement and uneven heating of the specimen, were addressed in this study.

Material

The composite used in this study was a six ply T650-35/AMB21 carbon fiber/polyimide laminate. The eight-harness satin fiber textile fabric was obtained from Amoco Performance Products Inc., while impregnation of the resin was performed by the Polymer Branch of the Materials Division at NASA Lewis Research Center (LeRC). The dimensions of the cut prepreg panels used for assembling the laminate were 30.48 × 30.48 cm (12 × 12 in.), with an average ply thickness of 0.0339 cm (0.0133 in.).

After stacking, the prepreg was placed into a preforming mold and staged for 1 hr at 204 °C (400 °F). Next, the stack was placed into a matched metal die. The composite was then molded by placing the die into a press heated to 316 °C (600 °F) and applying a pressure of 3.45 MPa (500 psi) when the die temperature had reached 232 °C (450 °F). After reaching 316 °C (600 °F), the pressure and temperature were maintained constant for 2 hr. The laminate was then cooled and removed from the mold when the temperature dropped to 232 °C (450 °F). Finally, the laminate was subjected to a post-cure treatment at 329 °C (625 °F) for 16 hr. The fiber volume content was 0.58 and the void content was 0.02 (values were provided by the Polymers Branch using the acid digestion technique (ref. 22)). Subsequently, the panels were water jet cut into dog-bone specimens and oven dried in air at 121 °C (250 °F) for 6 hr. To minimize moisture absorption, the specimens were stored in a desiccator until the time of testing.

The glass transition temperature, T_G, was measured as 305 °C (581 °F) using DuPont's thermo-mechanical analyzer (TMA) 800. TMA measures the linear expansion of a material as a function of temperature; the point at which an increase in the rate of expansion occurs denotes the T_G of the material. Figure 1 shows the normalized thickness expansion as a function of temperature. As can be seen in the figure, a change in slope occurs at approximately 305 °C (581 °F).

To verify the results from the TMA test, a rheological analysis was performed using the RMS 800, manufactured by Rheometrics Inc. The system measures the T_G by applying a sinusoidal oscillation, hence strain, to a specimen and measuring the resulting torque as a function of temperature. Computer analysis of the data calculates viscoelastic properties such as the storage modulus (G'), loss modulus (G"), and loss tangent (δ). The temperature at which G" and δ decrease while G' increases defines the T_G of the material. The graphical result of the rheological analysis for the T650-35/AMB21 cross-weave laminate is presented in figure 1(b). The T_G was found to be approximately 304 °C (579 °F), which was in good agreement with the TMA results.

A C-Scan of the post-cured plate exposed areas of varying attenuations indicating the possibility of defects. Further, subsequent to machining, inspections of the specimen edges with a magnifying glass revealed the presence of localized delaminations and pits on a number of specimens. Figure 2 displays typical pretest damage as seen by an edge view at 20x magnification (pits not shown in this figure). Given that the primary objective of this study was to develop elevated temperature experimental techniques for this class of materials, the questionable quality of the laminate was not a critical issue. However, this pre-existing damage will influence the experimental results and may contribute to the relatively high degree of scatter revealed under cyclic fatigue conditions.

Specimen Design

The specimen design employed in this study is shown in figure 3. This design was based on a modified version of a reduced gage section coupon utilized for high temperature testing of metal matrix composites (MMCs) and ceramic matrix composites (CMCs) (ref. 23). Shear stresses in the area of the radius are minimized by using a relatively small value for the curvature (large radius), thus creating a very gradual area reduction transition region.

The goal prior to testing was to use a 15.24 cm (6 in.) dog bone specimen without end tabs. For this study, two variations in the overall specimen length were examined for comparison; the 15.24 cm (6 in.) coupon and an elongated 17.78 cm (7.0 in.) specimen (fig. 3). The elongated geometry was exactly the same as the shorter coupon's except for an extension of material in the tab area.

After a few static tensile tests, it was concluded that the longer specimens were necessary if coupons without tabs were to be used. This was noted because of the repeated grip failures in the shorter specimen when tabs were not used. The longer coupons were successful because of the increased gripping area and lower hydraulic grip pressure required for preventing slip. The remaining 15.24 cm (6 in.) coupons were tabbed and utilized for the subsequent tests, although, for future studies only the longer specimens will be employed (see fig. 3 for tab details).

Equipment

The experiments were conducted under computer control on a closed-loop, servo-hydraulic test system with a 88.96 kN (20 kips) capacity (fig. 4). The fatigue test control software incorporated tensile and compressive stiffness measurements at periodic intervals. All mechanical tests were conducted in load control. Specimen gripping was accomplished through the use of water cooled hydraulic wedge grips.

Strain measurements were obtained by an air cooled 1.27 cm (0.5 in.) gage length extensometer mounted on the edge of the specimen. Contact with the coupon was achieved by using either flat chisel or V-chisel end probes made from high purity alumina. The tare force of each probe was approximately 2.9 N. Transverse strain measurements were made only for the room temperature static tensile tests using commercially available strain gauges.

The specimen was heated by using two banks of three high intensity tungsten-filament quartz bulbs (500 W/bulb) placed facing the width dimension of the specimen and oriented perpendicular to the loading axis as schematically shown in figure 5. Parabolic reflectors inside the lamp bodies focused the radiant energy

evenly onto the specimen. The single zone heating system was controlled by a self-tuning closed loop temperature controller. Adjustable support fixtures allowed the lamp bodies to be independently maneuvered facilitating the reduction of the temperature gradient over the gage section. Using this heating system, temperatures as high as 1500 °C (2732 °F) can be attained at 100 percent power in a matter of seconds. As was mentioned earlier, the dynamic capabilities of the quartz lamps make them the optimal energy source for future thermomechanical fatigue experiments.

Innovative test techniques needed to be developed for accurate temperature measurement when using radiant heating in conjunction with PMCs. For conductive materials, such as MMCs, thermocouples can be directly spot-welded onto the surface of the specimen to obtain the surface temperature (ref. 24). For obvious reasons, no such method of directly including the specimen in the circuit of the thermocouple is available for the nonconductive polymer materials. A technique utilized for CMCs, which are usually poor conductors, involves embedding a thermocouple into a bead of similar material and physically attaching the bead to the specimen (ref. 25).

A similar procedure was employed for the PMCs in this study. A K-type thermocouple was embedded in a pure PMR-15 block and physically attached to the coupon using a small stainless steel clip as shown in figure 6. A single block measurement was used for this study, although, the average temperature of two separate blocks on opposite faces could also have been utilized. By placing the block just outside of the gage section and employing a relatively small clip, the problem of shading from the block and clip was minimized. Because of the conductivity of carbon fibers and the potential interference it could have on the thermocouple current, only the resin material without the fibers was employed. PMR-15 was used because of its availability and comparable properties. The block shape was cubic with a side dimension of 0.254 cm (0.10 in.).

Due to the geometry and thermodynamic boundary condition differences between the block and the specimen, it was expected that the block temperature would not be equal to that of the coupon. This assumption was shown to be true by utilizing a calibration specimen with five internal thermocouples located in the center gage section of the coupon. The five thermocouples spanned a total length of 2.54 cm with a 0.635 cm spacing in-between. A relationship between internal coupon temperature and block temperature was achieved by stepping through various temperatures and correlating the two measurements. At each step of interest in the cycle, the lamp setting was maintained for a period of time to allow thermal equilibrium in both the block and the specimen. From these measurements, a correlation curve for this specific laminate lay-up was constructed (fig. 6). When conducting subsequent tests, an identical correlation block and specimen were placed in the exact same positions as in the calibration experiments.

The coupon with the internal thermocouples was also used for positioning the lamps for optimal gradients in the gage section. Once lamp positioning was completed, the maximum temperature was located at the center internal thermocouple. The readings at the gage section boundaries (±1.27 cm from center) were at most 3 °C below the center line temperature.

Test Details

The elevated test temperature (ET) selected for this study was 255 °C (491 °F). This temperature was 50 °C (90 °F) below the dry glass transition temperature, T_G, which was measured at 305 °C (581 °F). For each room temperature (RT) coupon, a pre-test modulus measurement was conducted, while for the ET experiments both RT and ET moduli were recorded. Specimens at the ET were allowed to soak for 2 min before load was applied. Based on the previous correlation experiments, this was sufficient time to allow for thermal equilibrium of the test coupon. In all cases the strain was zeroed after obtaining equilibrium temperature, hence only mechanical strains were recorded. On average, a static tensile test specimen was maintained at the ET for approximately 5 min from start to fracture.

A total of three static tensile tests were conducted at each of the two temperature conditions (RT and ET) with a load rate to failure of 6.9 kPa/sec (1 ksi/sec). Specimen failure, for both static and fatigue tests, was defined as complete fracture of the specimen into two pieces.

The isothermal fatigue experiments at 255 °C were conducted at three levels of maximum stress, S_{max}, with $R_\sigma = 0.1$ ($\sigma_{min}/\sigma_{max}$). The S_{max} values were based on the average ultimate tensile strength, σ_{ult}, at 255 °C (491 °F) obtained from the first part of this study. These values were 0.7 σ_{ult} (538 Mpa), 0.8 σ_{ult} (621 MPa), and 0.9 σ_{ult} (690 MPa). As a comparison, a set of isothermal fatigue tests were conducted at RT with a S_{max} value of 641 MPa, representing 0.8 times the RT σ_{ult}. Due to limitations related to extensometer contact with the specimen edge, a cyclic load frequency of 2 Hz with a triangular command wave form was

employed. At this rate sufficient extensometer probe contact was maintained. The triangular wave form facilitates deformation modeling by supplying a constant deformation rate.

RESULTS/DISCUSSION

Tensile Behavior

The results of the tensile tests are summarized in tables I and II. Typical deformation behaviors are displayed in figures 7 and 8. For this woven laminate, linear behavior was observed up to approximately 90 percent of the ultimate load. The nonlinearality in the final stages of loading was primarily due to fiber breaks and matrix cracking. Beyond the proportional limit, loud "popping" sounds were caused by the fiber bundles fracturing as the ultimate stress was approached. It appeared from the quasi-static tensile data that temperature had no effect on modulus or ultimate stress and strain, although more testing needs to be completed to give this statement statistical significance. Because of the fiber dominated behavior of the woven laminates, the strength was assumed to be maintained at the ET for these relatively short duration tensile tests. A similar conclusion about the strength of polyimide composites exposed to extreme temperatures for limited periods was reached when conducting tensile tests with nonwoven unidirectional carbon fiber/PMR-15 resin laminates (ref. 26).

Fatigue Behavior

Figure 9 describes the macroscopic isothermal fatigue behavior of the composite at 255 °C. Also shown for comparison in figure 9 are a limited number of experiments conducted at RT. As can be seen in the figure, the spread in cycles to failure is quite extensive at all stress levels. This excessively large variation was due to the initial poor quality of the composite as discussed previously. Even with the relatively high degree of scatter, the plot still reveals the general trend of increased life with decreasing maximum stress. Also, the data in figure 9 seems to show no difference in comparable lives for ET and RT at 0.8 σ_{ult}, although, no statements of statistical significance could be made due to the scatter and the small number of specimens.

Table III outlines isothermal fatigue and material properties of the specimens tested at ET and RT. Comparisons of the initial longitudinal moduli (tensile and compressive) with cycles to failure at the selected loads were made to see if a correlation existed; however, no correlation was apparent. Further, for each ET specimen the difference in initial moduli between the two temperature extremes ($E_{RT} - E_{ET}$) were plotted verses N_f. Here too, no correlation could be found. This was contrary to a past study where a higher initial longitudinal stiffness was an indication of higher strength and longer life (ref. 27). However, it is noteworthy to point out that the specimens tested in reference 27 were quasi-isotropic nonwoven graphite epoxy.

As the fibers broke during testing brooming occurred, especially along the edges (recall that probe contact points were on the edge). To minimize the influence of this fraying on the probe contact, various probe configurations were tried. The best results were obtained when using probes with flat chisel geometries. Conical point end probes were not examined in the present study, but will be evaluated in future efforts. For all conditions it was found that a small drop of Elmers® glue on each probe helped maintain contact even at 255 °C (491 °F).

The maximum composite strain at failure was plotted against N_f as shown in figure 10. In general, the trend obtained from the graph revealed that the maximum strain at (N_f) was within the scatter band of the static tensile ultimate strain, excluding the questionable 2 percent strain reading from a lone datum point. This result has also been documented in a previos study dealing with positive R-ratio fatigue and stiffness degradation as a damage metric (ref. 28).

A representative fatigue response of a T650-35/AMB21 cross-weave at 255 °C is shown in figure 11, where the maximum cyclic stress was 538 MPa (78 ksi) or 0.7 $\sigma_{ult\ 255\ °C}$. Multiple cycles are shown to illustrate the progressive changes in deformation behavior up to the cycle before failure. The mechanisms at work during the ratcheting process, or "walking" of the σ - ε curve during tension-tension fatigue, were assumed to involve physical damage (fiber and resin fracture), environmental attack on the resin (chemical degradation and mass loss), and viscoelastic deformation all of which were functions of time, load, and environment. Note that strain ratcheting also occurred at RT (not shown), and at a rate similar to that exhibited at ET. This trend seemed to suggest that strain accumulation due to environmental mechanisms had

limited impact on strain accumulation. More tests at various frequencies and temperatures need to be conducted to reinforce this observation.

Additionally, Figure 11 reveals that beyond initial cycles the deformation response showed a non-linear behavior. An actual stiffening with load occurred, creating a concave shape for the σ - ε curve. The upper half of the deformation curve decreased in stiffness in the first 10 percent of life. This was followed by an increase to levels close to initial values, followed again by a gradual decrease to failure. The unexpected increase in stiffness was probably due to the mechanism of straightening out and locking up of the longitudinal kinked fibers at higher loads. Figure 12 documents the stiffness change by displaying the loading and unloading moduli verses cycles. The loading moduli was defined as the slope of the line starting at S_{min} and ending at the halfway point on the load curve. The slope value of the unloading moduli was obtained from the line starting at S_{max} and ending at the midpoint of the unloading curve. In figures 11 and 12, it is shown that the deformation curves regained linear behavior as fiber lock-up was degraded by other damage mechanisms and the loading and unloading moduli merge.

Figure 13 displays typical strain behavior for the cross-weave of interest. It was noticed that three distinct regions were relevant. Within the first 10 percent of life, the strain accumulated at a relatively high rate followed by a second region identified by a long term shallow gain. Finally, a dramatic increase in strain occurred in the final 10 percent of the specimen's life and continued until failure. This three region trend in strain accumulation occurred in all RT and ET fatigue specimens and appeared to be a good indicator of the damage state.

Figure 14 shows the tensile and compressive moduli as a function of load cycles during isothermal fatigue. These values represent the moduli as measured from zero stress to ±35 MPa, respectively. The routine for periodically obtaining the data was implemented into the control software. As can be seen from the figure, the data showed a general trend of decreasing moduli.

It is to be stated that figures 11 to 14 show representative behaviors for all the coupons tested regardless of cyclic load level or temperature. It was observed that the trends in deformation response, strain accumulation, and moduli degradation were very similar for all fatigue conditions. In all cases damage accumulated at high rates in the first 10 percent and last 10 percent of life. Also, due to the poor quality of the laminate and the resulting scatter in data, the results are only trend indicators for composite materials under these conditions.

Finally, after completing all tensile and fatigue tests it was concluded that the 17.78 cm (7 in.) dog-bone geometry was required if testing without tabs is preferred. All of these specimens broke in the gage section once the appropriate grip pressure was used. The shortened 15.24 cm (6 in.) specimens were successful only when employing tabs.

SUMMARY/CONCLUSIONS

An investigation was conducted to develop experimental techniques for elevated temperature uniaxial mechanical testing of PMCs. To this end, the tensile and cyclic fatigue behaviors of a carbon/polyimide eight-harness satin weave system, T650-35/AMB21, were investigated. Because of the limited amount of material and the questionable quality of the plate, only the trends in behavior were studied. The following summarizes the major accomplishments and findings:

Experimental techniques;

(1) An untabbed, dog-bone specimen geometry was established, exhibiting consistent gage section failures under all test conditions.

(2) A technique for accurate temperature control and measurement when using radiant heating quartz lamps was developed and implemented.

(3) The issue of in-situ strain monitoring during cyclic fatigue at elevated temperature was solved using high temperature extensometry.

(4) Multiple methods were utilized to monitor fatigue damage during mechanical cycling. These included the in-situ σ - ε deformation behavior, real-time measurements of static tensile and compressive moduli, and changes in maximum/minimum strain.

Tensile and cyclic fatigue behavior of T650-35/AMB21 cross-weaves;

(5) The relatively short term static tensile and fatigue tests appeared to have shown that the properties were well maintained at the elevated temperature of interest, although, no statistical significance can be given to this statement due to scatter and the small number of specimens available. For the quasi-static tensile tests, both temperature conditions displayed nominally linear stress-strain behavior up to failure.

(6) Large variations in the macroscopic fatigue behavior of the laminates were noticed in the maximum stress verses life plots. The significance of these variations was attributed to the poor pretest quality of the laminate plate. The general trend of decreased life with increased load was maintained for the three maximum stress levels of 0.7, 0.8, and 0.9 σ_{ult} ($R_\sigma = 0.1$).

(7) Strain ratcheting occurred for all cases of the load controlled cyclic fatigue (RT and ET). Three distinct strain growth regions were realized in the tests. The first 10 percent and last 10 percent of life showed a relatively high rate of strain accumulation. In between these regions was an area of stable, slow strain accretion.

(8) The residual moduli and the accumulation of strain during cyclic fatigue were used as indicators of the damage state, although, the initial moduli gave no indication of the relative tensile strengths or cyclic fatigue lives.

ACKNOWLEDGEMENTS

The authors would like to thank Dr. G.D. Roberts of NASA Lewis Research Center and Mr. D.A. Scheiman of NYMA, Inc. for providing the results of the TMA and rheological analysis.

REFERENCES

1. Hahn, H.T.: "Fatigue Behavior and Life Prediction of Composite Laminates," *Composite Materials: Testing and Design (Fifth Conference), ASTM STP 674,* S.W. Tsai, Ed., American Society for Testing and Materials, 1979, pp. 383–417.
2. Norman, T.L., Civelek, T.S., and Prucz, J.: "Fatigue of Quasi-Isotropic Cylinders under Tension-Tension Loading," *Journal of Reinforced Plastics and Composites,* Vol. II, Nov. 1992.
3. Reifsnider, K.L., Schulte, K., and Duke, J.C.: "Long-Term Fatigue Behavior of Composite Materials," *Long Term Behavior of Composites, ASTM STP 813,* T.K. O'Brien, Ed., American Society for Testing and Materials, Philadelphia, 1983, pp. 136–159.
4. Curtis, P.T. and Moore, B.B.: "A Comparison of the Fatigue Performance of Woven and Non-Woven CFRP Laminates," RAE TR–85059, June, 1985.
5. Reifsnider, K.L.: Fatigue of Composite Materials, Elsevier Science Publishers B.V., Amsterdam, The Netherlands, 1991.
6. Stotler, C.L. and Yokel, S.A.: "PMR Graphite Engine Duct Development," Final Report, NASA CR–182228, August, 1989.
7. Herakovich, C.T., Davis, Jr., J.G., and Mills, J.S.: "Thermal Stresses in Severe Environments," New York, NY: Plenum Press, 1980.
8. Xiang, Z.D. and Jones, F.R.: "Thermal Degradation of an End-Capped Bismaleimide Resin Matrix (PMR–15) Composite Reinforced with PAN-Based Carbon Fibres," *Composites Science and Technology*, **47**, 1993, pp. 209–215.
9. Gyekenyesi, A., Hemann, J., and Binienda, W.: "Crack Development in Carbon/Polyimide Cross-ply Laminates Under Uniaxial Tension," *Sampe Journal*, Vol. 30, No. 3, May/June 1994.
10. Awerbuch, J., Perkinson, H.E., and Kamel, I.H.: "Deformation Characteristics and Failure Modes of Notched Graphite Polyimide Composites at Room and Elevated Temperatures," NASA CR–159375, Aug., 1980.
11. Cavano, P.J. and Winters, W.E.: "Fiber Reinforced PMR Polyimide Composites," NASA CR–135377, May, 1978.

12. Jones, C.J., Dickson, R.F., Adam, T., Reiter, H., and Harris, B.: "The Environmental Fatigue Behavior of Reinforced Plastics," *Proc. R. Soc., London,* A396 pp. 315–338 (1984).
13. Reed, S.M., Herakovich, C.T., and Sykes, G.F.: "The Effects of Space Radiation on a Chemically Modified Graphite-Epoxy Composite Material," NASA TM–89232, 1987.
14. Gates, T.S.: "Effects of Elevated Temperature on the Viscoplastic Modeling of Graphite/Polymeric Composites," *High Temperature and Environmental Effects on Polymeric Composites, ASTM STP 1174,* C.E. Harris and T.S. Gates, Eds., American Society for Testing and Materials, Philadelphia, 1993, pp. 201–221.
15. Hastie, R.L., Jr., and Morris, D.H.: "The Effects of Physical Aging on the Creep Response of a Thermoplastic Composite," *High Temperature and Environmental Effects on Polymeric Composites, ASTM STP 1174*, C.E. Harris and T.S. Gates, Eds., American Society for Testing and Materials, Philadelphia, 1993, pp. 163–185.
16. Adams, D.S., Bowles, D.E., and Herakovich, C.T.: "Thermally Induced Transverse Cracking in Graphite-Epoxy Cross-Ply Laminates," *Journal of Reinforced Plastics and Composites*, 5:152 (1986).
17. Camahort, J.L., Renhack, E.H., and Coons, W.C.: "Effects of Thermal Cycling Environment on Graphite/Epoxy Composites," *Environmental Effects on Advanced Composites Materials, ASTM STP 602*, Philadelphia, PA: ASTM (1976).
18. Harper, J., Whittenberger, J.D., and Hurwitz, F.I.: "Off-Axis Tensile Properties and Fracture in a Unidirectional Graphite/Polyimide Composite," *Polymer composites*, July, 1984, Vol. 5, No. 3.
19. Bae, H.R.: "Effects of Temperature on the Tensile Strength and Elastic Modulus of Composite Materials," M.S. Thesis, Naval Postgraduate School, March 1985.
20. Lo, Y.J., Liu, C.H., Hwang, D.G., Chang, J.F., Chen, J.C., Chen, Y.W., and Hsu, S.E.: "High Temperature Behaviors of an Innovative Polymeric Matrix Composite," *High Temperature and Environmental Effects on Polymeric Composites, ASTM STP 1174*, C.E. Harris and T.S. Gates, Eds., American Society for Testing and Materials, Philadelphia, 1993, pp. 66–77.
21. Strait, L.H.: "Thermomechanical Fatigue of Polymer Matrix Composites," The Pennsylvania State University Applied Research Laboratory, Technical Report No. TR 94–12, October, 1994.
22. Vannucci, R.: NASA LeRC, Private communication.
23. Worthem, D.W.: "Flat Tensile Specimen Design for Advanced Composites," NASA CR–185261, Nov., 1990.
24. Castelli, M.G., Bartolotta, P.A., and Ellis, J.R.: "Thermomechanical Testing of High Temperature Composites: Thermomechanical Fatigue (TMF) Behaviour of SiC (SCS-6)/Ti-15-3," *Composite Materials Testing and Design (Tenth Volume), ASTM STP 1120*, Glenn C. Grimes, Ed., American Society for Testing and Materials, Philadelphia, 1992, pp. 70–86.
25. Butkis, L.M.: "Thermomechanical Fatigue Behavior of a Silicon Carbide Fiber-Reinforced Calcium Aluminosilicate Glass-Ceramic Matrix Composite," Master's Thesis, The University of Michigan, 1991.
26. DiGiovanni, P.R. and Paterson, D.: "High Temperature, Short Term Tensile Strength of C6000/PMR–15 Graphite Polyimide," *Structures, Structural Dynamics and Materials Conference,* New Orleans, Louisiana, May 10–12, 1982, pp. 487–492.
27. Hahn, H.T. and Hwang, D.G.: "Failure Characterization of a Graphite/Epoxy Laminate Through Proof Testing," *Composite Materials: Testing and Design (Sixth Conference), ASTM STP 787*, I.M. Daniel, Ed., American Society for Testing and Materials, 1982, pp. 247–273.
28. Hwang, W. and Han, K.S.: "Fatigue of Composite Materials-Damage Model and Life Prediction," *Composite Materials: Fatigue and Fracture, Second Volume, ASTM STP 1012*, Paul A. Lagace, Ed., American Society for Testing and Materials, Philadelphia, 1989, pp. 87–102.

TABLE I.—STATIC TENSILE PROPERTIES OF
T650-35/AMB-21 CROSS-WEAVES AT 255 °C

Specimen ID	σ_{ult},	σ_{uult},	E_{LT} at 22 °C,	E_{LT} at 255 °C,
B1	827	1.40	65.2	65.0
B2	745	1.26	67.3	66.0
B3	745	1.23	69.4	68.7
Average	772	1.30	67.3	66.7
Stnd Dev	47	0.09	2.1	2.0

TABLE II.—STATIC TENSILE PROPERTIES OF
T650-35/AMB-21 CROSS-WEAVES AT 22 °

Specimen ID	σ_{ult},	ε_{ult},	E_{LT} at 22 °C, GPa	ν_{LT}
B5	779	1.43	70.9	0.044
B6	807	1.05	72.7	0.041
B7	814	1.17	71.9	0.048
Average	800	1.16	71.8	0.044
Stnd Dev	19	0.11	0.9	0.004

TABLE III. ISOTHERMAL FATIGUE AND MATERIAL PROPERTIES OF T650-35/AMB-21 CROSS-WEAVES

Test	Specimen	S_{max},	Initial $E_{22\ °C}$,[a]	Initial $E_{255\ °C}$,[a]	N_f,
255	A10	538 (0.7 σ_{ult})	62.3	61.7	1189090
"	B11	538	70.3	68.2	130497
"	B12	538	73.8	72.7	533083
"	A6	621 (0.8 σ_{ult})	57.3	56.4	11581
"	A7	621	64.3	63.4	467593
"	B13	621	68.8	67.3	11
"	A8	690 (0.9 σ_{ult})	64.8	63.0	6551
"	A9	690	70.9	70.0	76534
"	B9	690	71.3	67.2	52
"	B10	690	68.5	67.7	1
"	Average	----------	67.2	65.7	------
"	Stnd Dev	----------	5.0	4.7	------
22	B8	641 (0.8 σ_{ult})	71.2	—	13252
"	A3	641	68.0	—	8392
"	A5	641	71.1	—	262421
"	Average	----------	70.1	----	--------
"	Stnd Dev	----------	1.8	----	--------

[a] These values are longitudinal tensile moduli at 22 °C and 255 °C. Compressive moduli showed nearly the same magnitude and similar relationships between room and elevated temperatures.

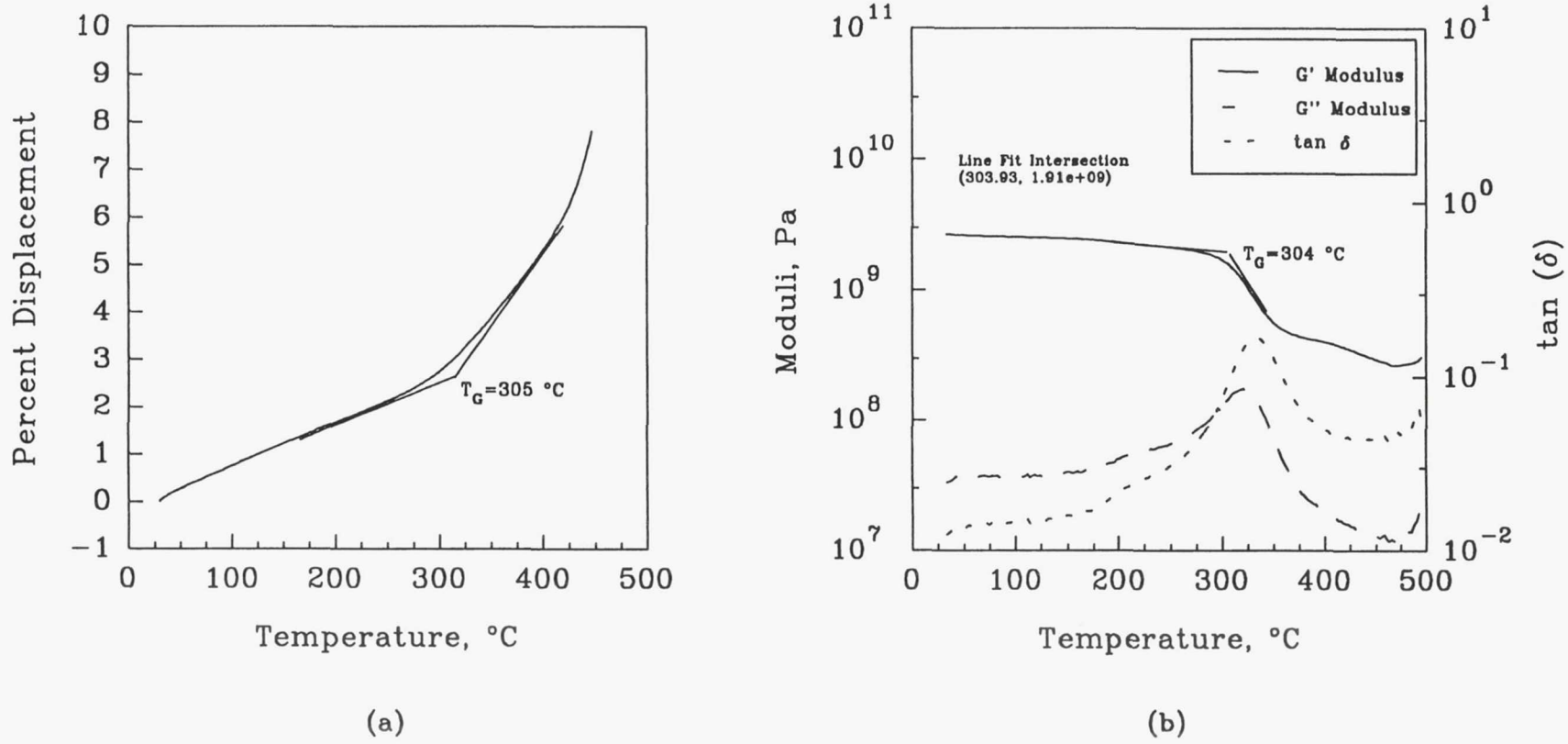

Figure 1.—Graphical results for obtaining T_G for T650–35/AMB21 cross-weave laminate using: (a) thermomechanical analyzer and (b) rheological analysis.

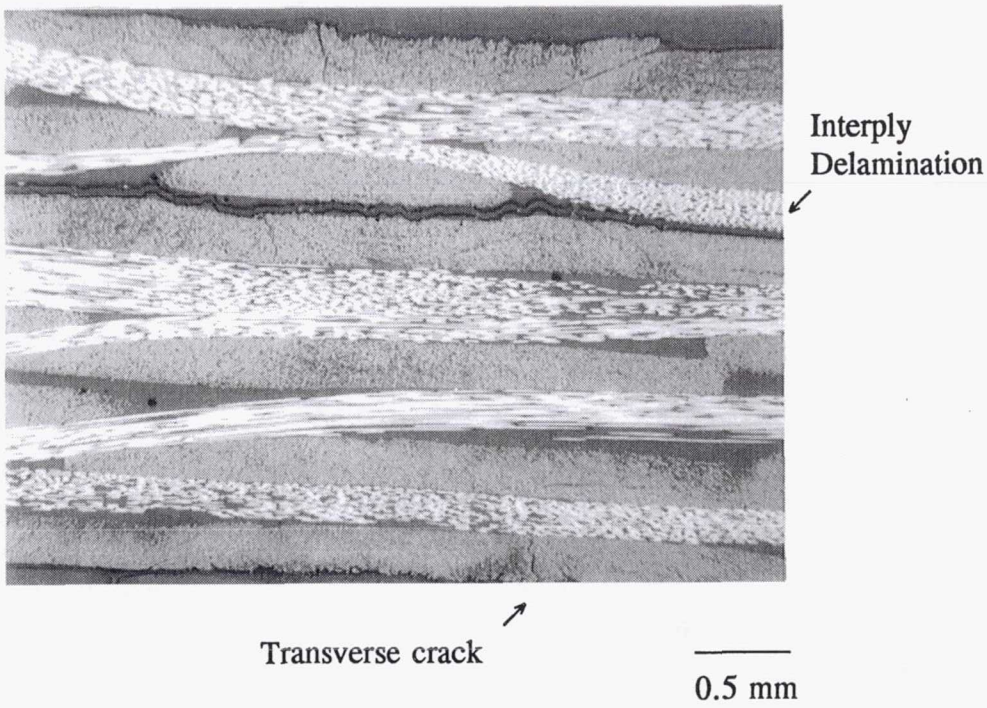

Figure 2.—Typical edge view of T650–35/AMB21 6-ply cross-weave showing pretest damage. (20x magnification)

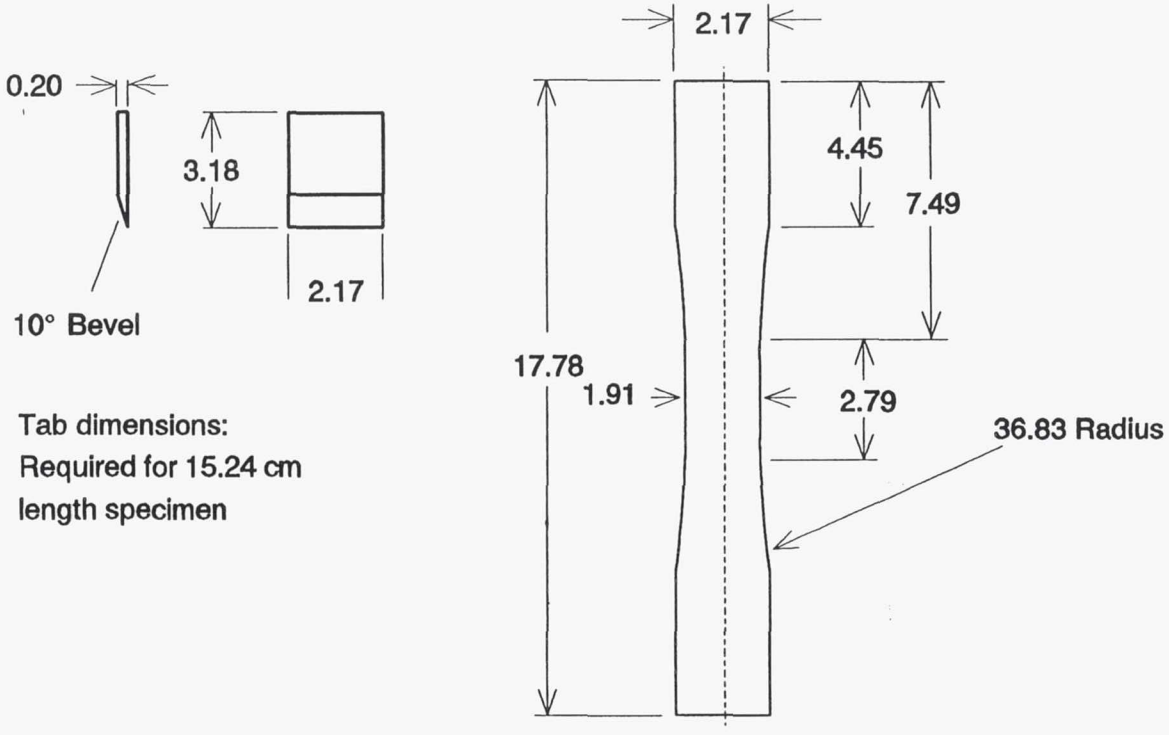

Figure 3.—Schematic of 17.78 cm (7 in.) length specimen design. (Dimensions in centimeters)

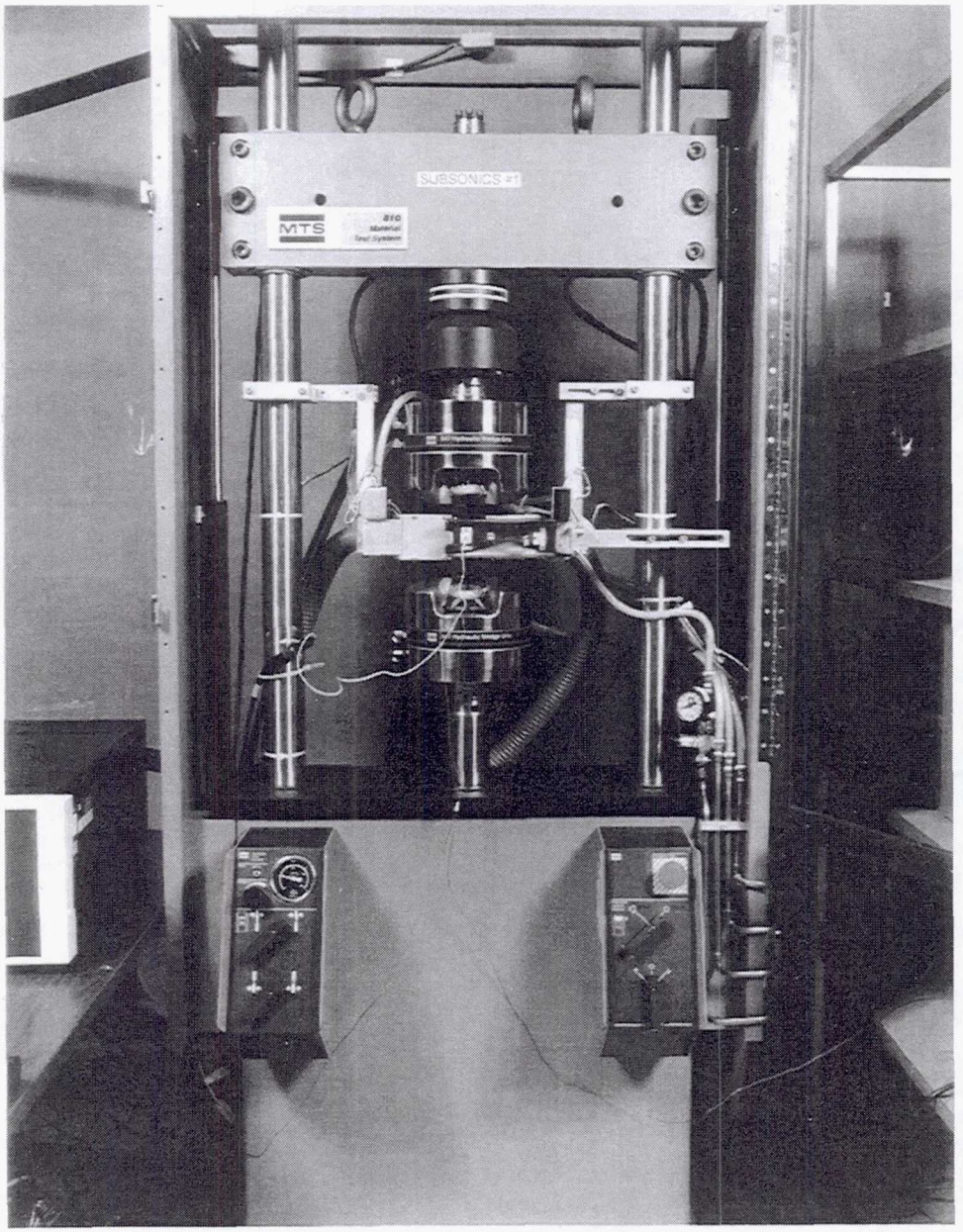

Figure 4.—Uniaxial composite test system.

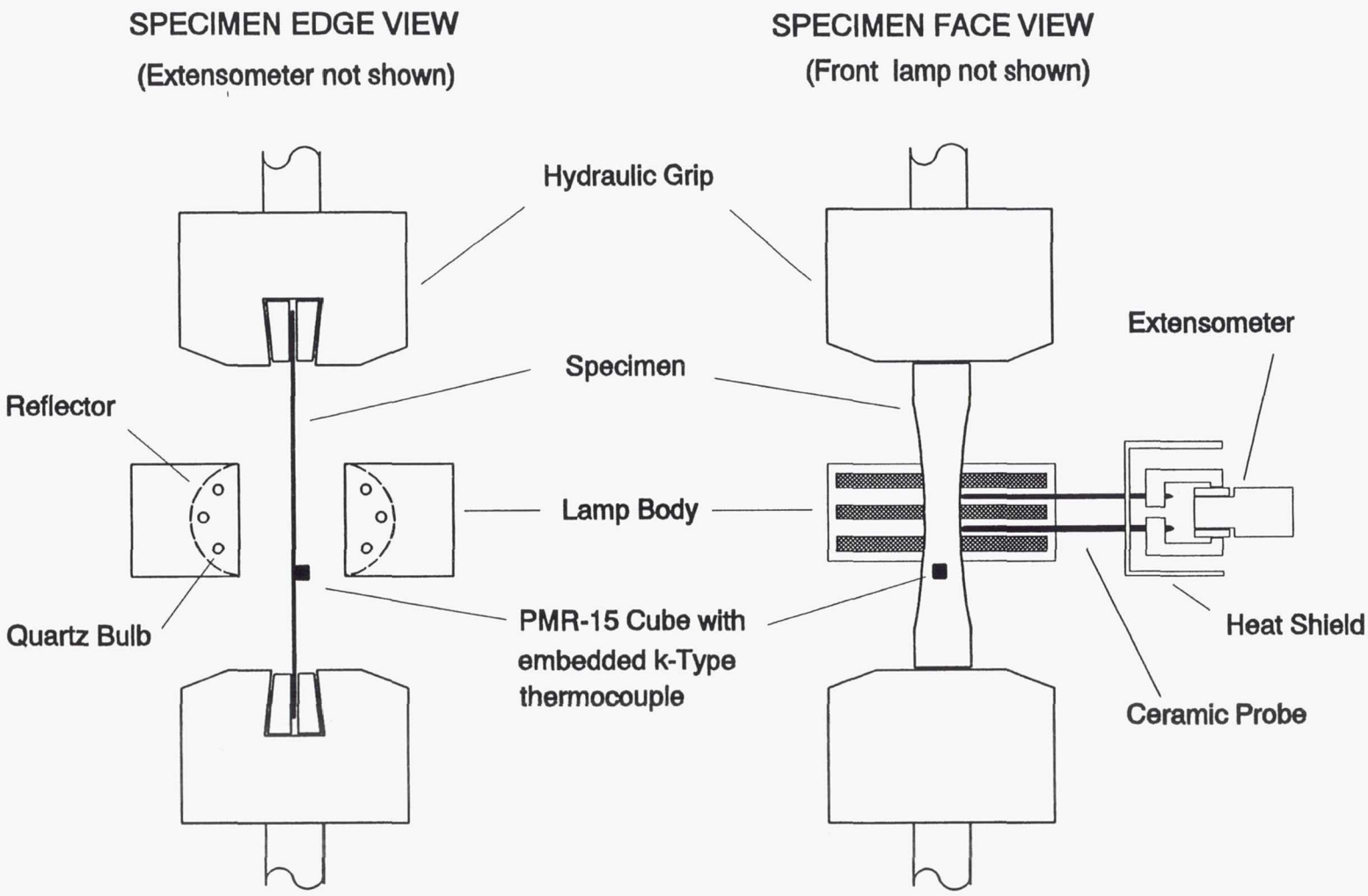

Figure 5.—Schematic view of specimen, quartz lamps, and extensometer.

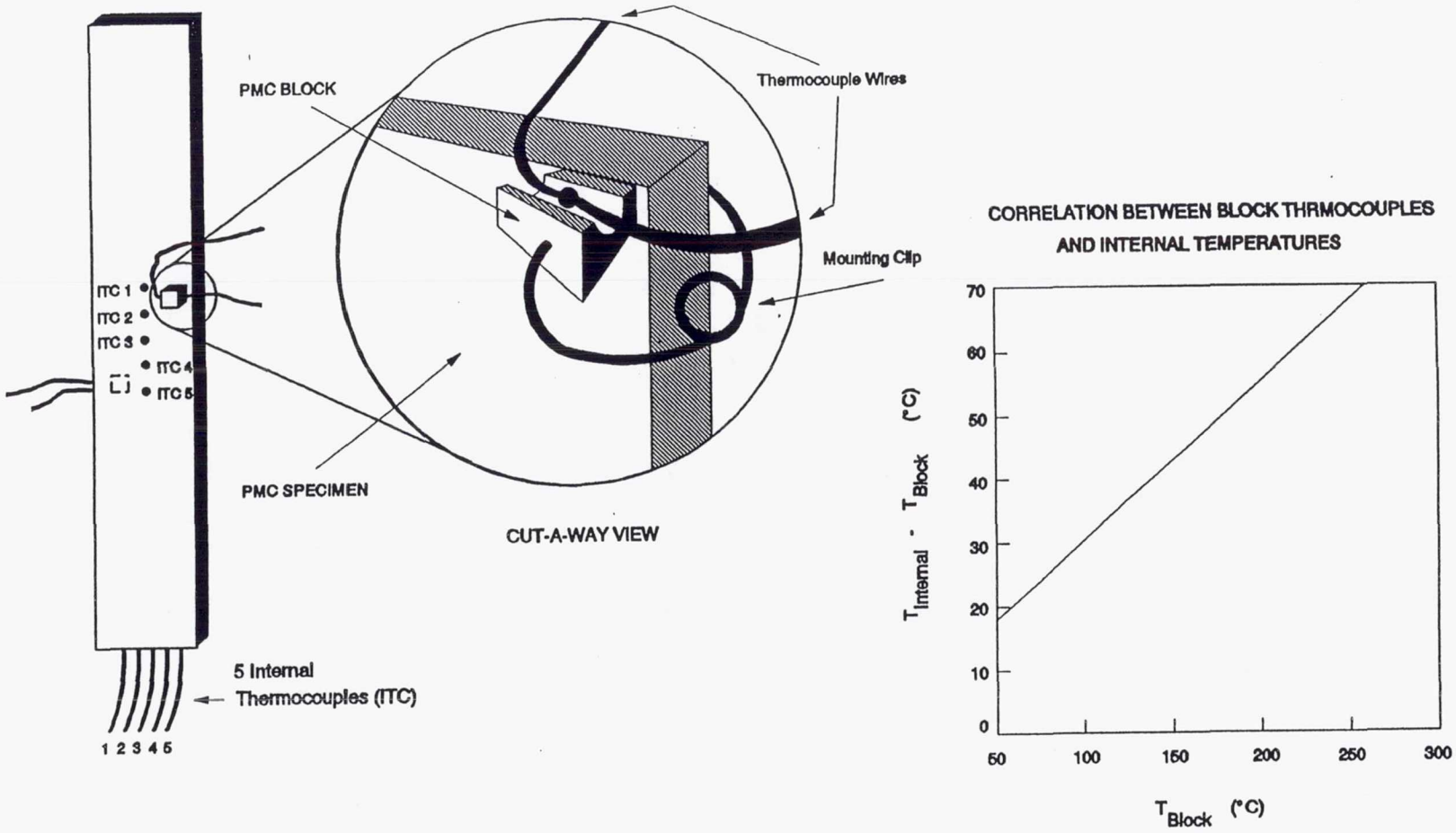

Figure 6.—Schematic of thermocouple block and correlation curve.

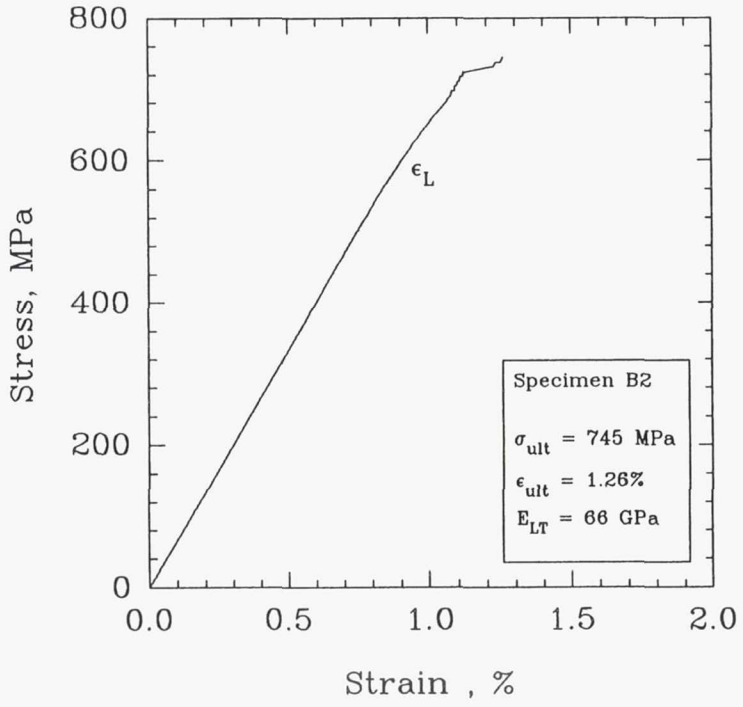

Figure 7.—Typical tensile response of T650–35/AMB21 6-ply cross-weave at 255 °C.

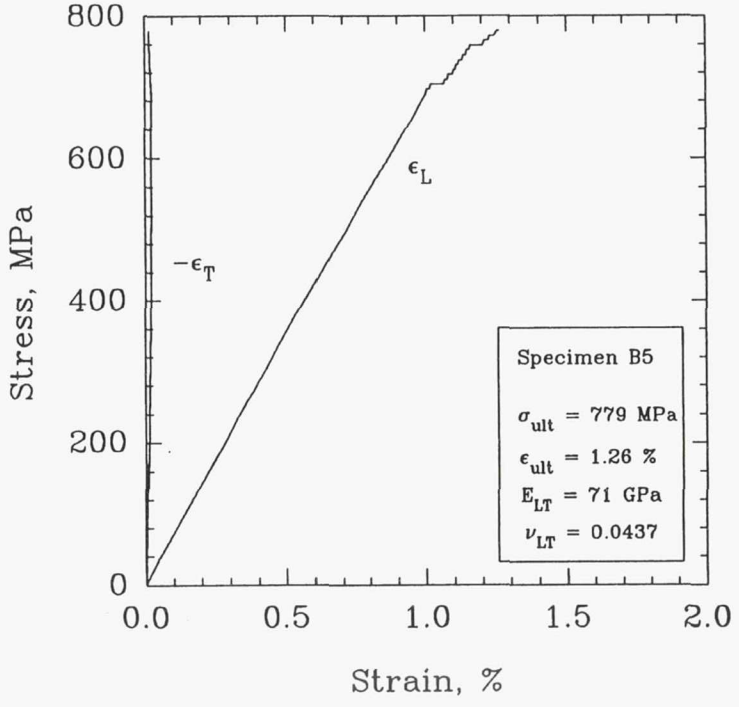

Figure 8.—Typical tensile response of T650–35/AMB21 6-ply cross-weave at 24 °C.

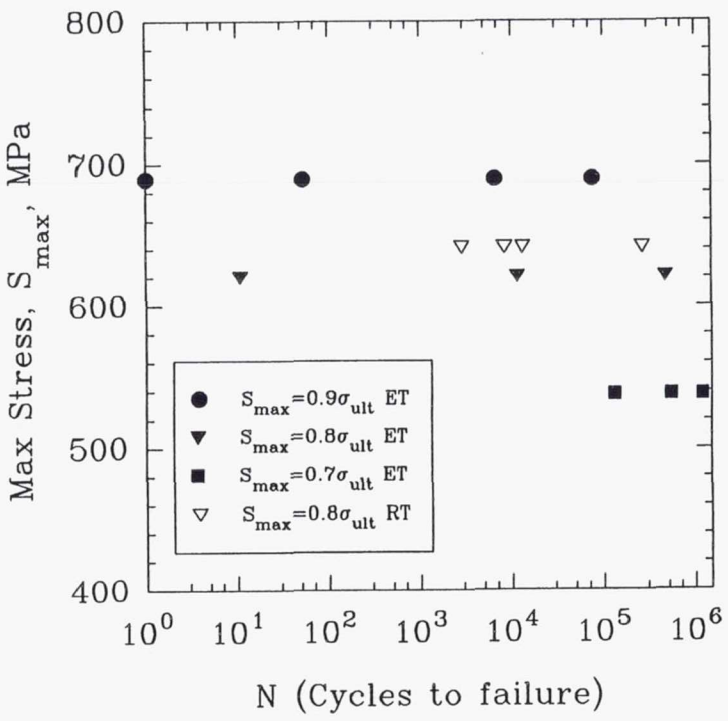

Figure 9.—Stress based isothermal fatigue life comparison for T650–35/AMB21 cross-weaves at 24 °C and 255 °C.

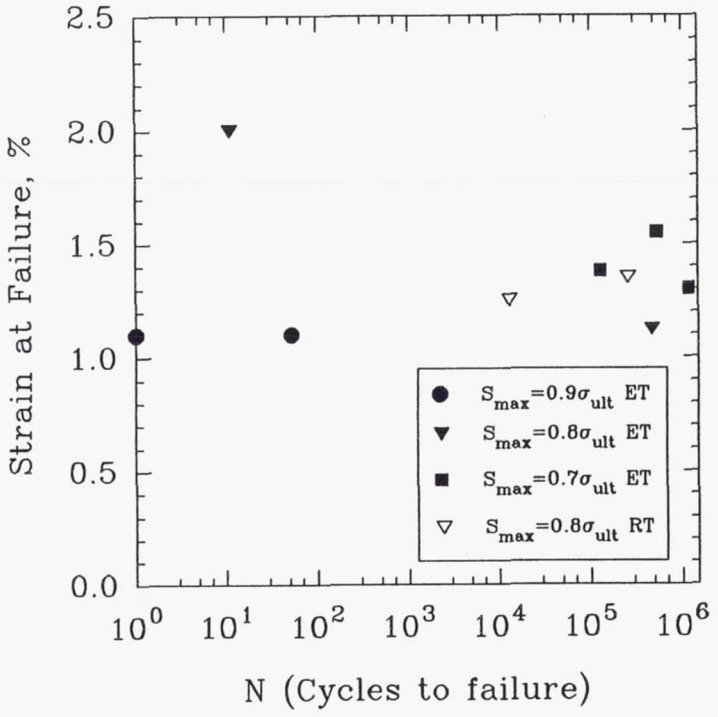

Figure 10.—Maximum mechanical strain values verses cycles to failure of T650–35/AMB21 6-ply cross-weaves at 24 °C and 255 °C.

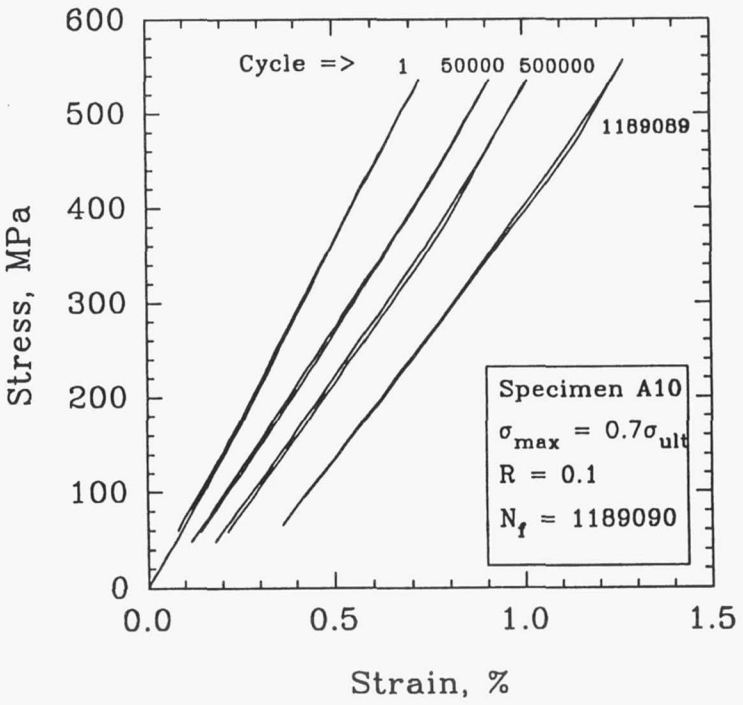

Figure 11.—Deformation response of T650–35/AMB21 6-ply cross-weave at 255 °C.

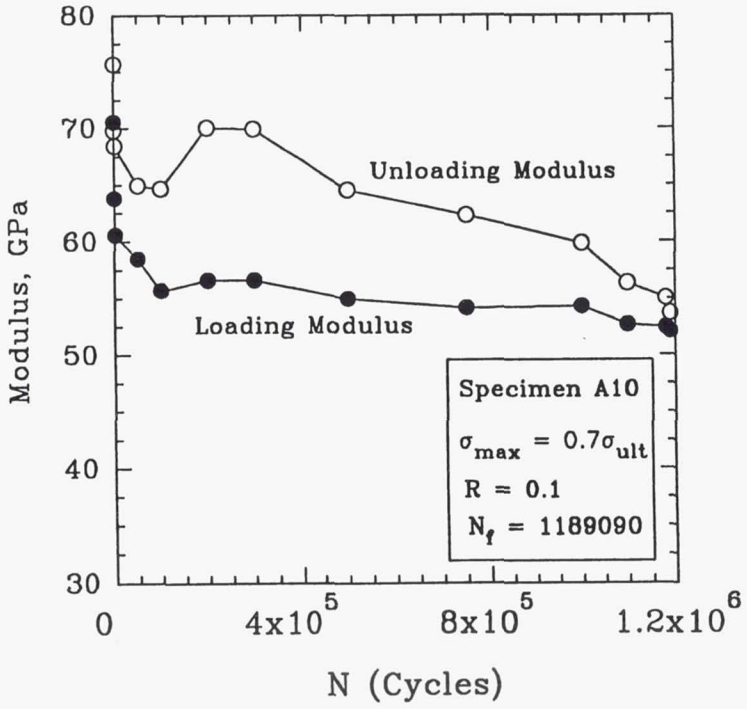

Figure 12.—Degradation of the 255 °C loading and unloading moduli during 255 °C isothermal fatigue of T650–35/AMB21 cross-weave.

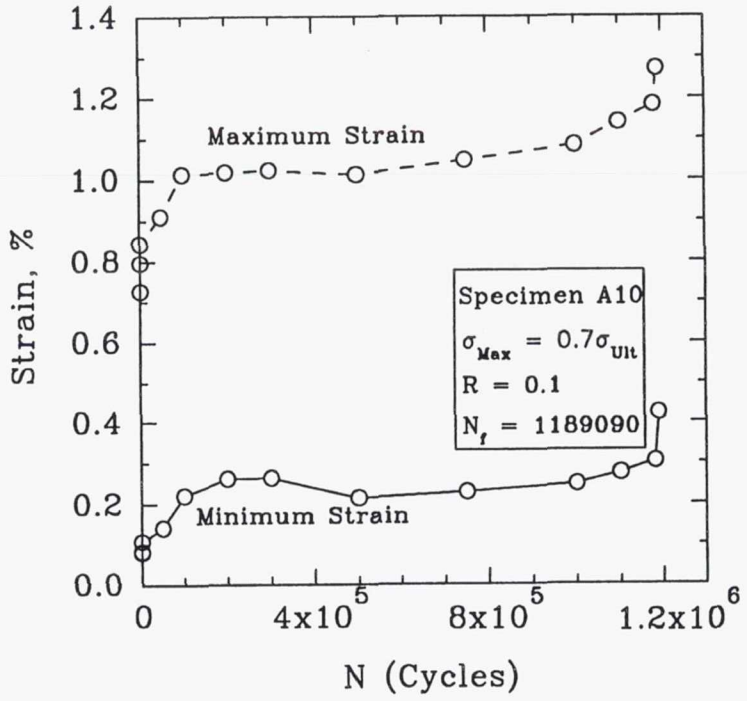

Figure 13.—Typical ratcheting behavior of T650–35/AMB21 cross-weave during isothermal fatigue at 255 °C.

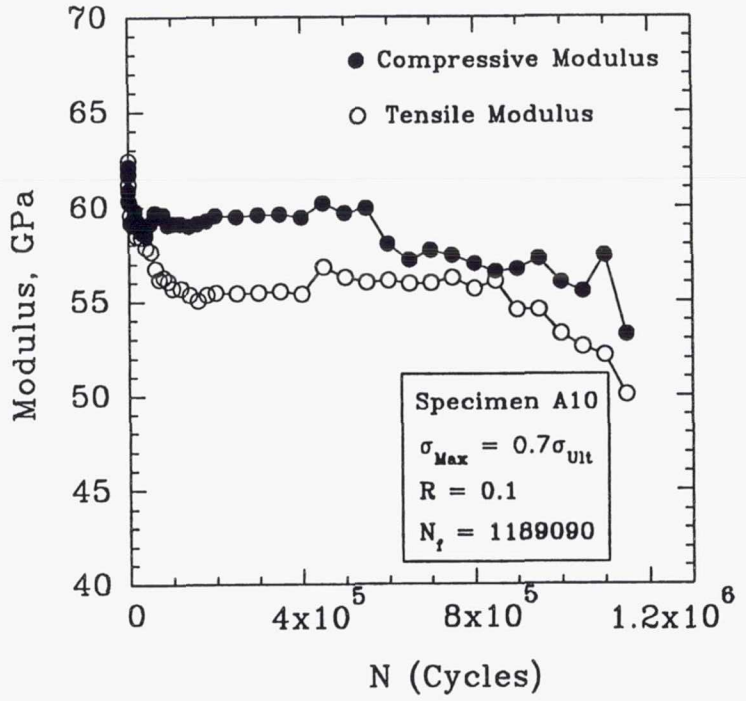

Figure 14.—Degradation of the 255 °C tensile and compressive static moduli during isothermal fatigue of T650–35/AMB21 cross-weave.

REPORT DOCUMENTATION PAGE

Form Approved
OMB No. 0704-0188

1. AGENCY USE ONLY (Leave blank)	2. REPORT DATE	3. REPORT TYPE AND DATES COVERED
	July 1995	Technical Memorandum

4. TITLE AND SUBTITLE

A Study of Elevated Temperature Testing Techniques for the Fatigue Behavior of PMCS: Application to T650-35/AMB21

5. FUNDING NUMBERS

WU-538-06-15

6. AUTHOR(S)

Andrew L. Gyekenyesi, Michael G. Castelli, John R. Ellis,
and Christopher S. Burke

7. PERFORMING ORGANIZATION NAME(S) AND ADDRESS(ES)

National Aeronautics and Space Administration
Lewis Research Center
Cleveland, Ohio 44135-3191

8. PERFORMING ORGANIZATION REPORT NUMBER

E-9648

9. SPONSORING/MONITORING AGENCY NAME(S) AND ADDRESS(ES)

National Aeronautics and Space Administration
Washington, D.C. 20546-0001

10. SPONSORING/MONITORING AGENCY REPORT NUMBER

NASA TM-106927

11. SUPPLEMENTARY NOTES

Andrew L. Gyekenyesi, Cleveland State University, Cleveland, Ohio 44115; Michael G. Castelli and Christopher S. Burke, NYMA, Inc., 2001 Aerospace Parkway, Brook Park, Ohio 44142 (work funded by NASA Contract NAS3-27186); John R. Ellis, NASA Lewis Research Center. Responsible person, John R. Ellis, organization code 5220, (216) 433-3340.

12a. DISTRIBUTION/AVAILABILITY STATEMENT

Unclassified - Unlimited
Subject Categories 24 and 07

This publication is available from the NASA Center for Aerospace Information, (301) 621-0390.

12b. DISTRIBUTION CODE

13. ABSTRACT *(Maximum 200 words)*

An experimental study was conducted to investigate the mechanical behavior of a T650-35/AMB21 eight-harness satin weave polymer composite system. Emphasis was placed on the development and refinement of techniques used in elevated temperature uniaxial PMC testing. Issues such as specimen design, gripping, strain measurement, and temperature control and measurement were addressed. Quasi-static tensile and fatigue properties (R_σ=0.1) were examined at room and elevated temperatures. Stiffness degradation and strain accumulation during fatigue cycling were recorded to monitor damage progression and provide insight for future analytical modeling efforts. Accomplishments included an untabbed dog-bone specimen design which consistently failed in the gage section, accurate temperature control and assessment, and continuous in-situ strain measurement capability during fatigue loading at elevated temperatures. Finally, strain accumulation and stiffness degradation during fatigue cycling appeared to be good indicators of damage progression.

14. SUBJECT TERMS

Carbon fiber/polyimide matrix composite; Fatigue behavior; Elevated temperature; Stiffness degradation; Quartz lamp heating

15. NUMBER OF PAGES

22

16. PRICE CODE

A03

17. SECURITY CLASSIFICATION OF REPORT	18. SECURITY CLASSIFICATION OF THIS PAGE	19. SECURITY CLASSIFICATION OF ABSTRACT	20. LIMITATION OF ABSTRACT
Unclassified	Unclassified	Unclassified	